Microbial Pathogenesis 220 (2026) 108809

Contents lists available at ScienceDirect

Microbial Pathogenesis

journal homepage: www.elsevier.com/locate/micpath

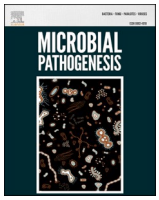

Evaluation and validation of reference genes for RT-qPCR analysis in different tissues of *Echinococcus multilocularis*-infected mice

Rui Chen, Meng Yin, Jian Xue, Jianhai Yin, Hua Liu, Congshan Liu *

National Institute of Parasitic Diseases, Chinese Center for Disease Control and Prevention, Chinese Center for Tropical Diseases Research, National Key Laboratory of Intelligent Tracking and Forecasting for Infectious Diseases, Key Laboratory of Parasite and Vector Biology, National Health Commission of the People's Republic of China, WHO Collaborating Centre for Tropical Diseases, National Center for International Research on Tropical Diseases, Ministry of Science and Technology, Shanghai, 200025, China

ARTICLE INFO

Keywords:
Echinococcus multilocularis
Reference gene
Internal control
Liver
Lung
Spleen
RT-qPCR

ABSTRACT

Echinococcosis, caused by the larval stage of the tapeworm *Echinococcus* species, threatens global public health and livestock economics. Currently, quantitative reverse transcription polymerase chain reaction (RT-qPCR) is essential for mRNA quantification, and its accuracy relies on stably expressed reference genes that must be validated under specific experimental conditions. In this study, we systematically evaluated the expression stability of twelve candidate reference genes in the liver, lung, and spleen of *E. multilocularis*-infected and healthy controls (n = 6 per group). Based on raw cycle threshold (Ct) values generated by RT-qPCR, the stability of each candidate gene was evaluated using both unstratified (samples from the same tissue were treated as a single cohort) and stratified (samples grouped by experimental condition) strategies. Then multiple algorithms including NormFinder, geNorm, BestKeeper, and Delta-Ct were employed to generate a comprehensive stability ranking of candidate genes. The validated optimal reference gene combinations were subsequently used to normalize gene expression via the comparative Ct ($2^{-\Delta\Delta Ct}$) method. Our findings demonstrated that optimal reference genes were tissue-specific under *E. multilocularis* infection. For example, stratified analysis identified *Actb* as the most stable in both the liver (stability value = 0.16) and lung (stability value = 0.29), and *Rpl13a* (stability value = 0.10) in the spleen. Consequently, distinct reference gene combinations were validated and recommended respectively for liver, lung, and spleen, providing a reliable basis for accurate gene expression analysis by RT-qPCR. The reference sets will facilitate future investigations into echinococcosis, including disease pathogenesis, antiparasitic drug efficacy assessment, and therapeutic target discovery.

1. Introduction

Echinococcosis, also known as hydatid disease, is a zoonotic parasitic disease caused by the larval stages of tapeworms of the genus *Echinococcus* [1]. Cystic echinococcosis (CE) and alveolar echinococcosis (AE), caused by *E. granulosus* sensu lato and *E. multilocularis*, respectively, are the two most clinically significant forms of echinococcosis, imposing a substantial burden on public health and the livestock industry [2]. CE is globally distributed whereas AE is predominantly prevalent in the Northern Hemisphere [1]. Human infection occurs through the accidental ingestion of *Echinococcus* eggs, mainly via contaminated food or water, and hand-to-mouth transmission [3,4]. Following intestinal hatching, oncospheres penetrate the intestinal wall, enter the circulation, and subsequently develop into metacestodes predominantly in the liver (>70% of cases) and lungs, and less frequently in the spleen and other organs [5–8]. In particular, AE is characterized by malignant, tumor-like infiltrative growth and accounts for approximately 0.66 million disability-adjusted life years globally, with a mortality rate exceeding 90% within 10-15 years of diagnosis in untreated or inadequately treated patients [2,9,10]. Surgical and chemotherapeutic treatments with benzimidazoles (albendazole and mebendazole) remain the primary options for the clinical management of echinococcosis [2,3]. However, treatments remain challenging owing to limited therapeutic options, poor cure rates of existing drugs, and their associated adverse effects [11,12]. Therefore, elucidating the pathogenic mechanisms underlying AE is essential for the development of novel therapeutic

* Corresponding author. National Institute of Parasitic Diseases, Chinese Center for Disease Control and Prevention (Chinese Center for Tropical Diseases Research), Shanghai, 200025, China.
E-mail address: liucs@nipd.chinacdc.cn (C. Liu).

https://doi.org/10.1016/j.micpath.2026.108809
Received 11 June 2026; Received in revised form 13 August 2026; Accepted 25 August 2026
Available online 26 August 2026

approaches.

As a crucial molecular biology technique, reverse transcription quantitative PCR (RT-qPCR) enables sensitive, specific, and high-throughput quantification of gene expression dynamics, thereby facilitating the elucidation of complex signaling networks that regulate diverse cellular responses under various pathological conditions [13]. During AE infection, stage-dependent differential gene expression patterns have been revealed in host tissues using RT-qPCR analysis: the early and middle stages were characterized by active cell cycle progression and proliferation, whereas the late stage exhibited a shift toward cell cycle arrest and apoptosis [14]. Furthermore, this technique has also provided valuable insights into the mechanisms of action of anti-echinococcal drugs. For example, it revealed an anti-inflammatory cytokine profile in bone marrow-derived dendritic cells, which partially resulted the ineffectiveness of resveratrol in *E. granulosus* infected animals [15].

The accuracy and reliability of RT-qPCR critically depend on normalization with stably expressed reference genes, typically housekeeping genes [16]. However, extensive studies have revealed that some conventionally employed housekeeping genes displayed inconsistent expression patterns across distinct tissues and pathological conditions [17,18]. Accordingly, considerable efforts have been devoted to validating candidate reference genes under specific experimental conditions to identify the most stably expressed ones for normalization. For instance, in metabolic disease models such as high-fat diet induced obesity or caloric restriction, TATA-box binding protein (*Tbp*), peptidylprolyl isomerase A (*Ppia*), hydroxymethylbilane synthase (*Hmbs*), and beta-2 microglobulin (*β2m*) were identified as stable reference genes [19,20]; similarly, ribosomal protein L32 (*Rpl32*), *Hmbs,* 14-3-3 protein zeta (*Ywhaz*), glyceraldehyde-3-phosphate dehydrogenase (*Gapdh*), and succinate dehydrogenase complex flavoprotein subunit A (*Sdha*) were proved to be stably expressed in host tissues during gastrointestinal nematode infections [21,22]. To identify stably expressed reference genes suitable for normalizing target gene expression, NormFinder, geNorm, BestKeeper, and the Delta Ct are widely used, each relying on distinct underlying principles and algorithms. Among them, NormFinder employs an analysis of variance (ANOVA)-based model that simultaneously estimates intra- and inter-group variations [23]; geNorm determines stability by calculating the average pairwise variation (M value) of each gene with all other candidates [24]; BestKeeper performs a descriptive statistical analysis directly on raw Ct values, assessing expression stability based on standard deviation (SD) and coefficient of variation (CV) [25]; and the Delta-Ct method ranks genes according to the standard deviation of delta-Ct (ΔCt) values across all samples [26].

In studies of *Echinococcus* infection, *Gapdh* and beta-actin (*Actb*) have been widely used as reference genes for RT-qPCR analysis in *Echinococcus*-infected mouse models [14,27–29]. However, given that *E. multilocularis* infection profoundly alters host metabolic and immune homeostasis [30], whether these genes remain stably expressed during infection is unclear, and any infection -induced variation in their expression could introduce substantial bias into RT-qPCR quantification. Therefore, in the present study, the expression stability of seventeen commonly used housekeeping genes, including *β2m*, *Ppia*, tubulin beta-2A class lla (*Tubb2a*), ribosomal protein lateral stalk subunit P0 (*Rplp0*), 18S ribosomal RNA (*Rn18s*), mitochondrial ribosomal protein L32 (*Mrpl32*), *Gapdh*, beta-glucuronidase (*Gusb*), alpha-tubulin (*Tuba*), hypoxanthine guanine phosphoribosyl transferase (*Hprt*), ribosomal protein L13A (*Rpl13a*), beta-actin (*Actb)*, *Ywhaz*, transferrin receptor (*Tfrc*), *Tbp*, *Hmbs* and phosphoglycerate kinase 1 (*Pgk1*) in the liver, lungs, and spleen tissues from *E. multilocularis*-infected mice were systematically investigated for the first time, by integrating algorithmic rankings. These validated reference gene sets establish a reliable foundation for an accurate RT-qPCR based gene expression analysis, paving the way for subsequent mechanistic exploration.

2. Materials and methods

2.1. Parasites, animals and tissue collection

Twelve female BALB/c mice (four weeks old) were purchased from SLAC Laboratory Animal Center (Shanghai, China) and randomly assigned into two groups: (1) *E. multilocularis*-infected group, each mouse received an intraperitoneal injection of 2000 viable *E. multilocularis* protoscoleces [31]; (2) Control group, mice were administered an equal volume of sterile physiological saline via the same route. These animals were housed in a specific-pathogen-free facility under controlled conditions (temperature 23 ± 1 °C, 12:12 h light-dark cycle). After six months of infection, all animals were anesthetized. At the end of the experiment, the mice were weighed, and cysts were dissected from the infected animals, washed, and weighed.

Liver, lung, and spleen tissues were rapidly dissected, snap-frozen in liquid nitrogen, and stored at −80 °C until use. For each *E. multilocularis*-infected mice, liver samples were collected as: (1) perilesional tissue (PLT, ~5 mm^3, 1 mm of the macroscopic lesion border), and (2) distant tissue (DT, ~5 mm^3, within histologically confirmed non-infected liver tissue >5 mm far from the macroscopic lesion). Entire lung and spleen tissue (5 mm^3) collected from *E. multilocularis*-infected mice were represented as infected tissues (IT). Normal tissues (NT) from healthy subjects were used as control.

Animal procedures were carried out in compliance with the Guidelines for the Care and Use of Laboratory Animals produced by the Shanghai Veterinary Research Institute. The study was approved by the Ethics Committee of the National Institute of Parasitic Diseases, Chinese Center for Disease Control and Prevention (license number: IPD-2024-019).

2.2. Histopathological examination of E. multilocularis-infected liver tissues

Histopathological examination (hematoxylin and eosin staining, H&E) was performed on PLT, DT, and NT of the liver. Briefly, tissue samples were washed twice with ice-cold phosphate-buffered saline (G4202-500 ml, Servicebio, Wuhan, Hubei, China) and fixed in 4% neutral buffered formalin (G1101-15 ml, Servicebio, Wuhan, Hubei) at 4 °C for 48 h. Following fixation, samples were dehydrated through an ascending ethanol series (70%, 80%, 95%, and 100%, 100092683, Sinopharm Chemical Reagent Co.Ltd., Shanghai, China), cleared in xylene (X100301-S5L, Shanghai Lingfeng Chemical Reagents Co., Ltd., Shanghai, China), embedded in paraffin (SWE-JBL5, Servicebio, Wuhan, Hubei, China), and stained with H&E (G1076, Servicebio, Wuhan, Hubei, China) for microscopic examination.

2.3. RNA extraction and quality control

Total RNA was extracted using the SPARKeasy Cell RNA Rapid Extraction Kit (AC0205-A, SparkJade, Jinan, Shandong, China) following the manufacturer's instructions. The residual genomic DNA was removed by DNase I treatment (SM0371, Thermo Fisher Scientific, Waltham, MA, USA). RNA concentration and purity were assessed using a NanoDrop spectrophotometer (Thermo Fisher Scientific, Waltham, MA, USA). RNA samples with A260/A280 ratios of 1.9-2.2 and A260/A230 ratios ≥2.0 were used for further analysis. RNA integrity was confirmed by 1% agarose gel electrophoresis.

2.4. Reverse transcription quantitative PCR

First-strand cDNA was synthesized from 1 μg of total RNA with random hexamer oligonucleotide primers in a 20 μL reverse transcription system (RR047A, Takara Bio, Kusatsu, Shiga, Japan). Reverse transcription was performed at 37 °C for 15 min, followed by enzyme inactivation at 85 °C for 5 s. The prepared cDNA was stored at −20 °C

until use.

Seventeen housekeeping genes commonly used as internal control genes in mice were selected, and the primer sequences were designed according to previously published literature [19,20]. Oligonucleotide primers were synthesized by Sangon Biotech Co., Ltd. (Shanghai, China) (Table 1).

RT-qPCR was performed on a CFX96 Touch Real-Time PCR Detection System (Bio-Rad, Hercules, CA, USA) using TB Green Premix Ex Taq II (RR820A, Takara Bio, Kusatsu, Japan). Each 25 μL reaction system contained 12.5 μL of 4×TB Green Premix, 2 μL of cDNA template, 1 μL each of the forward and reverse primers (10 μM), and 8.5 μL of nuclease-free water. The amplification program consisted of initial denaturation at 95 °C for 30 s, followed by 40 cycles of denaturation at 95 °C for 5 s and primer annealing at 60 °C for 10 s, and extension at 72 °C for 30 s. Melting curve analysis was subsequently performed by heating from 65 °C to 95 °C (0.5 °C increments) with continuous fluorescence monitoring to verify amplification specificity. In addition, the RT-qPCR products were validated by 5% agarose gel electrophoresis (Supplementary Fig. S1). Each sample was run in duplicate technical replicates, with Ct values showing a standard deviation (SD) < 0.2. No-template controls were included in each run to monitor potential contamination.

RT-qPCR amplification efficiency (E) was determined for each primer pair using standard curves generated from ten-fold serial dilutions of pooled cDNA. For each serial dilution, mean Ct values were plotted against the logarithm of the cDNA dilution factor. E values were calculated according to the equation: $E = 10^{(-1/slope)}-1$ [32,33], where the slope was obtained from the linear regression line. The coefficient of determination (R^2) values derived from standard curves were used to validate the linearity (Supplementary Fig. S1). Subsequently, twelve out of seventeen candidate reference genes were retained for subsequent stability analysis, based on the following criteria: E values between 90% and 110%, and $R^2 \geq 0.99$ (Table 1).

2.5. Determination of optimal reference genes

For unstratified analysis (assessing overall expression stability without distinguishing between infected and control groups), mean raw Ct values were analyzed using RefFinder (https://blooge.cn/RefFinder/), which integrates NormFinder [23], geNorm [24], BestKeeper [25], and the comparative Delta-Ct method [26], and finally generates consensus rankings. For stratified analysis, which included pairwise comparisons of experimental groups and a global analysis across all experimental groups, raw Ct values were linearized via the $2^{(-Ct)}$ transformation, then analyzed using NormFinder (version 0.953, MOMA, Aarhus University Hospital, Aarhus, Denmark). Both intra-sample (unstratified) and inter-group (stratified) analysis comprehensively rank stabilities of candidate gene, and identify the optimal reference gene combinations for normalization: in the unstratified analysis, the top two genes from the consensus ranking were selected as the normalization pair, as the algorithm did not provide

Table 1
Primer information of seventeen candidate reference genes for RT-qPCR.

Gene Symbol	Gene Name	Function	Primer Sequence (5′ to 3′)	Amplicon Size (bp)	Amplification Efficiency (E, %)	Correlation Coefficients (R^2)	Whether selected as reference genes
β2m	Beta-2 microglobulin	Antigen presentation	F: CATGGCTCGCTCGGTGAC R: CAGTTCAGTATGTTCGGCTTCC	135	100.2	1.000	Yes
Ppia	Peptidylprolyl isomerase A	Protein folding catalyzing	F: CAAACACAAACGGTTCCCAG R: TTCACCTTCCCAAAGACCAC	85	92.0	0.999	Yes
Tubb2a	Tubulin beta-2A class lla	Microtubule polymerization	F: CTTAGTGAACTTCTGTTGTCCTCCAGCA R: AGGCAAACTGAGCACCATAATTTACAAA	68	93.4	0.997	Yes
Rplp0	Ribosomal protein lateral stalk subunit P0	Translation elongation	F: GGCCCTGCACTCTCGCTTTC R: TGCCAGGACGCGCTTGT	124	92.3	0.992	Yes
Rn18s	18S ribosomal RNA	Ribosomal subunit assembly	F: GCGAATGGCTCATTAAATCAGTTA R: TGGTTTTGATCTGATAAATGCACG	150	92.1	0.999	Yes
Mrpl32	Mitochondrial ribosomal protein L32	Mitochondrial translation	F: AGGTGCTGGGAGCTGCTACA R: AAAGCGACTCCAGCTCTGCT	51	93.3	0.999	Yes
Gapdh	Glyceraldehyde-3-phosphate dehydrogenase	NAD-dependent glyceraldehyde-3-phosphate oxidation	F: TGCACCACCAACTGCTTAG R: GGATGCAGGGATGATGTTC	177	91.9	0.996	Yes
Gusb	Beta-glucuronidase	Lysosomal enzyme degrades glycosaminoglycans	F: CCGACCTCTCGAACAACCG R: GCTTCCCGTTCATACCACACC	169	94.8	0.999	Yes
Tuba	Alpha tubulin	Microtubule nucleation and stability	F: TGTCCTGGACAGGATTCGC R: CTCCATCAGCAGGGAGGTG	115	100.3	0.999	Yes
Hprt	Hypoxanthine guanine phosphoribosyl transferase	Purine salvage enzyme involved in nucleotide metabolism	F: TGGATACAGGCCAGACTTTGTT R: CAGATTCAACTTGCGCTCATC	124	107.3	0.997	Yes
Rpl13a	Ribosomal protein L13A	Translational elongation	F: AGGGGCAGGTTCTGGTATTG R: TGTTGATGCCTTCACAGCGT	120	92.9	0.998	Yes
Actb	Beta-actin	Cytoskeletal dynamics and cell motility	F: CATTGCTGACAGGATGCAGAAGG R: TGCTGGAAGGTGGACAGTGAGG	138	92.6	0.998	Yes
Ywhaz	14-3-3 protein zeta	Phosphoserine-dependent signaling adaptor	F: GAAAAGTTCTTGATCCCCAATGC R: TGTGACTGGTCCACAATTCCTT	134	88.8	0.999	No (E value out of range)
Tfrc	Transferrin receptor	Iron homeostasis via endocytosis	F: AGACCTTGCACTCTTTGGACATG R: GGTGTGTATGGATCACCAGTTCCTA	70	148.8	0.981	No (E value out of range)
Tbp	TATA-box binding protein	Transcription initiation	F: CCTTGTACCCTTCACCAATGAC R: ACAGCCAAGATTCACGGTAGA	119	144.9	0.986	No (E value out of range)
Hmbs	Hydroxymethylbilane synthase	Heme biosynthesis	F: ATGAGGGTGATTCGAGTGGG R: TTGTCTCCCGTGGTGGACATA	134	82.8	0.995	No (E value out of range)
Pgk1	Phosphoglycerate kinase 1	ATP generation in glycolysis	F: ATGTCGCTTTCCAACAAGCTG R: GCTCCATTGTCCAAGCAGAAT	164	83.5	0.999	No (E value out of range)

specific combination recommendations; in the stratified analysis, the optimal two gene combination recommended by the algorithm was directly employed as the normalization pair.

2.6. Relative expression analysis of candidate reference genes

The relative expression levels of target genes were calculated using the $2^{-\Delta\Delta Ct}$ method to compare the expression of housekeeping genes between experimental groups [26]. To minimize variations and enhance reliability, the geometric mean of the reference gene pair recommended by the unstratified and stratified methods was used as the normalization factor for each sample, rather than a single reference gene [24].

2.7. Statistical analysis

An unpaired two-tailed Student's t-test or non-parametric Mann-Whitney *U* test was used to compare group means according to the data distribution. Data were presented as mean ± standard deviation (SD). All analyses were conducted using GraphPad Prism 10.4.1 (GraphPad Software, San Diego, CA, USA). Statistical significance was set at $P < 0.05$.

3. Results

3.1. Characterization of E. multilocularis-infected mouse model

After six months of infection, *E. multilocularis* cysts were observed in the livers of these animals (Fig. 1), while no visible lesion was found in spleen or lung tissues. These cysts were measured 0.8-1.5 cm in diameter and weighed 1.57 ± 0.89 g, whereas no significant differences in body weights of animals were observed between experimental groups ($t = 0.1531$, $P = 0.8813$) (Fig. 1, Table 2).

Histopathological examination revealed intact lobular architectures with regular hepatocyte arrangement and no pathological changes in NT (Fig. 2). In contrast, a characteristic periparasitic granuloma with extensive collagen deposition and lymphocytic infiltration, complete architectural disruption, and diffuse fibrous tissue proliferation, was observed in PLT (Fig. 2). In addition, DT showed diffuse hepatocellular vacuolation with mildly dilated sinusoids. (Fig. 2).

3.2. Ct values profiling of liver, lung and spleen tissues

Overall, the candidate reference genes displayed similar expression patterns across tissues, as exemplified by *Rn18s,* which exhibited the lowest Ct values, whereas *Gusb* consistently displayed the highest Ct values (particularly in spleen tissue with Ct of 32.3 ± 1.7) (Fig. 3). However, tissue-dependent expression patterns were observed for some genes. For example, *β2m* exhibited higher expression in liver tissue (Ct values: 17.91 ± 1.1) than in the lung and the spleen (Ct values: 23.74 ± 3.2 and 24.66 ± 2.4, respectively) (Fig. 3). Moreover, Ct values of *β2m* were relatively consistent across biological replicates in the liver, whereas marked inter-sample variation of this gene was observed in

Table 2
Characteristics of *E. multilocularis*-infected and healthy experimental mice.

Group	Body Weights (g)	Age (weeks)	Cyst Weights (g)	Cyst Size (cm)	Numbers of Samples
E. multilocularis-infected	27.1 ± 2.0	28	1.57 ± 0.89	0.8 - 1.5	6
Control	27.0 ± 1.6	28	NA	NA	6

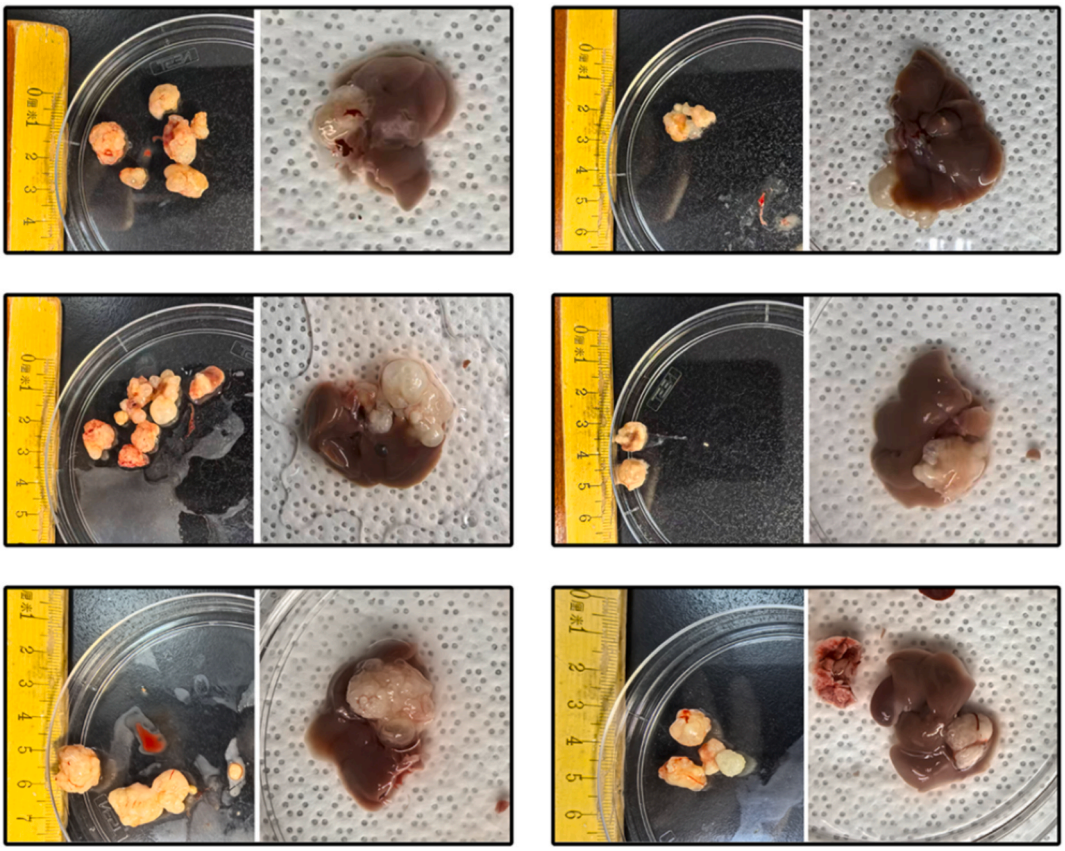

Fig. 1. Isolated *E. multilocularis* cysts and infected liver tissue at six months post-infection. Each image represents one experimental animal. The left panel shows *E. multilocularis* cysts collected from the infected liver; the right panel displays their original localization in the infected liver.

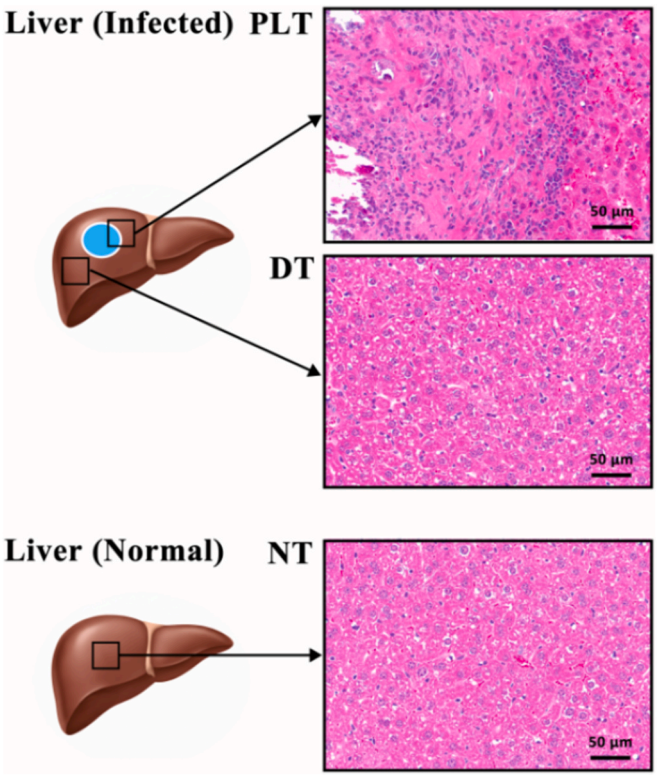

Fig. 2. H & E staining of mouse liver from healthy control and *E. multilocularis*-infected groups.

lung and spleen tissues (Fig. 3).

Notably, the inter-sample variations in gene expression displayed distinct patterns between infected and uninfected groups, as well as between the PLT and DT groups (Fig. 3). For example, *Mrpl32* exhibited the greatest variation in the liver but remained relatively stable in the lung and the spleen. In contrast, *β2m* displayed the largest inter-sample variation in lung and spleen tissues than in liver tissues.

3.3. Selection of optimal reference genes by ranking analysis

In unstratified analysis, samples derived from the same tissue were not stratified by group but were evaluated collectively. For liver tissues, *Rpl13a* and *Actb* were identified as the most stable genes using NormFinder and Delta-Ct algorithms, while *Ppia* and *Tuba, Actb* and *Tuba* were ranked the highest by geNorm and BestKeeper, respectively. Finally, based on the Consensus analysis, *Tuba* and *Actb* were recommended as the gene pair for normalization in the liver (Table 3). Moreover, *Rn18s* was ranked as the least stable gene in the liver by all algorithms except BestKeeper (ranked *Hprt* as the least stable gene). In lung tissues, the stably expressed *Tuba* and *Actb*, *Tubb2a* and *Ppia* were identified by geNorm and BestKeeper, respectively, while *Actb* and *Tubb2a* were ranked as the most stably expressed genes by NormFinder, Delta-Ct and the Consensus analysis. Moreover, *β2m* or *Hprt* was identified as the least stable gene in the lung. For spleen tissues, the ranking of stable genes varied across the four algorithms: NormFinder placed *Rpl13a* and *Tuba*, geNorm identified *Ppia* and *Mrpl32*, BestKeeper ranked *Tuba* and *Rpl13a,* and Delta-Ct selected *Actb* and *Mrpl32* at the top of stable genes. Integrating these results, the Consensus ranking designated *Actb* and *Mrpl32* as the most stable combinations. Moreover, *β2m* or *Rn18s* was identified as the least stable gene in the spleen.

In stratified samples, lung and spleen tissues were divided into NT and IT, while liver tissues were stratified into NT, PLT and DT, respectively (Table 4). For liver tissues, in the NT versus PLT comparison, *Actb* and *Rpl13a* were identified as the two most stable genes, but the reference gene pair combination recommended by NormFinder was *Gusb* and *Rpl13a.* When comparing NT with DT, *Rpl13a* and *Actb* were selected to be the most stable genes and best combination. In addition, *Rpl13a* and *Ppia* were identified as the most stable candidate genes in PLT versus DT comparison, but the reference gene pair combination recommended by NormFinder was *Rpl13a* and *Actb*. In addition, *Rplp0, Hprt* and *Rn18s* were identified as the least stable genes for these three comparisons, respectively. Moreover, when all three groups (NT, PLT and DT) were compared simultaneously in a single analysis, *Actb* and *Rpl13a* were selected as the two most stable genes, but the recommended reference gene pair combination was *Tuba* and *Rpl13a,* with Rn18s as the most unstable gene. For lung and spleen tissues, the recommended reference gene combinations in the NT versus IT comparison were *Actb* and *Tuba* (lung), and *Tuba* and *Rpl13a* (spleen), whilst *β2m* was identified as the least stable gene.

3.4. Relative quantification of candidate housekeeping genes normalized by recommended reference gene combination

To further characterize the expression profiles of the reference genes used in this study and to validate the performance of the selected reference gene combinations, normalization was performed using the optimal gene pairs identified by both the unstratified and stratified strategies (Fig. 4). In the liver, after using *Actb* and *Tuba* recommended by unstratified analysis as the internal reference across different infection states, it was found that *Ppia*, *Gusb* and *Rpl13a* which were listed among the top three ranked genes than genes (such as *Tubb2a*, *Rplp0, Rn18s, Mrpl32, Gapdh* and *Hprt*) which were ranked as one of the bottom-ranked genes (Fig. 4A). In addition, *Rplp0* and *Hprt* showed significant differences between NT and PLT groups ($t = 3.068$, $P = 0.0119$; $t = 2.263$, $P = 0.0471$, respectively) (Fig. 4A). Although no significant differences in the expression levels of *Tubb2a* ($U = 17$, $P = 0.9372$), *Rn18s* ($t = 0.9555$, $P = 0.3777$), and *Gapdh* ($t = 1.651$, $P = 0.1297$) were found between NT and PLT, substantial inter-sample variations was observed (Fig. 4A). In stratified analysis, the higher-ranked genes also exhibited greater expression stability than the lower-ranked candidates. In addition, *Rplp0* showed significant differences between NT and PLT (*Gusb* - *Rpl13a* as reference: $t = 2.719$, $P = 0.0216$; *Tuba* - *Rpl13a* as reference: $t = 2.97$, $P = 0.01318$) (Fig. 4A).

In lung tissues, using *Tubb2a* and *Actb* (recommended by unstratified analysis) or *Tuba* and *Actb* (recommended by stratified analysis) showed that housekeeping genes at the top ranking, such as *Tuba* and *Tubb2a*, also exhibited stable expression, while lower-ranked *β2m, Gusb,* and *Hprt* exhibited expression variations between NT and IT. In addition, *Rplp0* ($t = 2.462$, $P = 0.0336$) and *Mrpl32* ($t = 2.461$, $P = 0.0336$) exhibited significant differences between experimental groups (Fig. 4B). For spleen tissues, using *Mrpl32* and *Actb* (recommended by unstratified analysis) or *Tuba* and *Rpl13a* (recommended by stratified analysis) as the internal reference, the stable expression of top three tanked genes such as *Tuba*, *Actb*, *Rpl13a* and *Mrpl32,* as well as the variable expression of *β2m, Rn18s* and *Gusb* that contributed by the inter-sample variation were confirmed (Fig. 4C).

Comparison of stably and unstably expressed genes across tissues revealed that *Tuba* and *Actb* were consistently stable in all three tissues examined (Fig. 4D). Additionally, certain genes were specifically stable in individual tissues, such as *Ppia* and *Gusb* in the liver, *Mrpl32* in the spleen, and *Tubb2a* in the lung. In contrast, the least stable genes exhibited considerable inter-tissue variability. For example, four genes (*Mrpl32*, *Tubb2a*, *Rplp0* and *Gapdh*) were uniquely variable in the liver.

Finally, in *E. multilocularis*-infected mouse liver, we recommend the combination of *Tuba* - *Actb* or *Tuba* - *Rpl13a* as the optimal normalization factor. In addition, *Actb* - *Tubb2a* or *Actb* - *Tuba* are suitable options for lung tissues, while *Actb* - *Mrpl32* or *Rpl13a* - *Tuba* are recommended in spleen tissues.

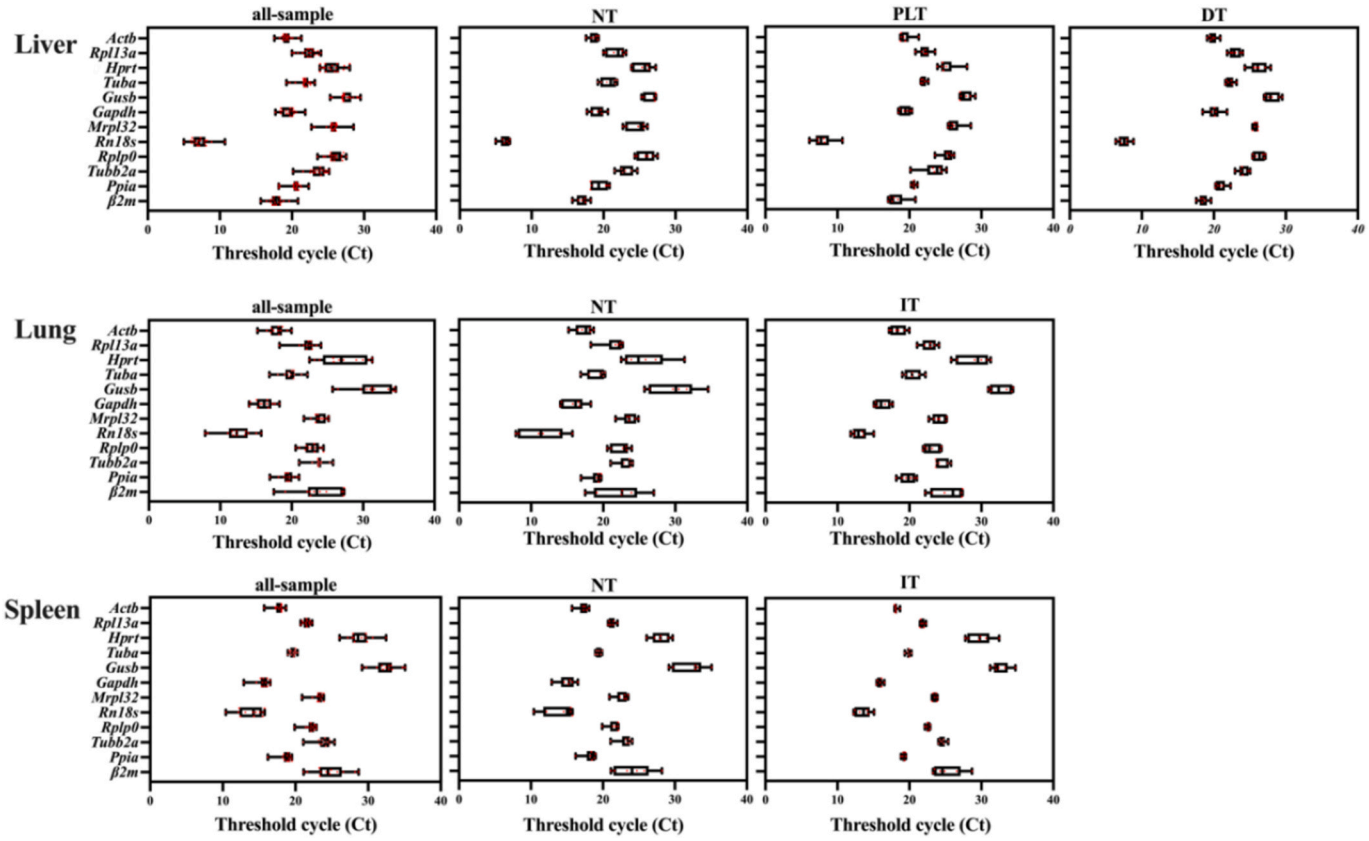

Fig. 3. Ct values of candidate reference genes in the liver, spleen, and lung tissues from *E. multilocularis*-infected and healthy mice. The box spans from the 25th to the 75th percentile. The whiskers extend to the minimum and maximum values. The vertical line inside the box indicates the median. Ct values of individual biological replicates. all-samples: all samples of liver, lung, and spleen, respectively; NT: normal tissues from healthy mice; IT: lung or spleen samples from *E. multilocularis*-infected mice; PLT: perilesional tissue of infected liver; DT: distant tissue of infected liver.

4. Discussion

In the present study, the expression stability of 12 candidate reference genes across liver, lung, and spleen tissues from *E. multilocularis*-infected mice was assessed by integrating algorithmic rankings. Our results demonstrated that parasitic infection significantly affected the expression of several housekeeping genes, rendering them unsuitable as internal controls. However, a subset of genes exhibited relatively stable expression across conditions in three tissues, including *Actb* and *Tuba,* which are two classical and widely used housekeeping genes in murine studies [34,35]. These genes encode the core cytoskeletal components beta-actin (microfilaments) and alpha-tubulin (microtubules), respectively, and are ubiquitously expressed in nearly all eukaryotic cell types. Consequently, they have long been assumed to be reference genes [36–38], although several reports have indicated that their expression stability is tissue-specific [39–41]. Our study further validated the stable expression of these two genes during *E. multilocularis* infection, providing evidence supporting their use as endogenous controls in this disease context, notably, *Actb* has already been applied as a reference gene in several previous studies [34].

In addition, several genes were confirmed to be stably expressed in specific tissues during this parasitic infection, including *Rpl13a*, *Ppia* and *Gusb* in the liver, *Rpl13a* and *Mrpl32* in the spleen, and *Tubb2a* in the lung. Some of these genes have also been reported to be stably expressed in other studies. For example, *Rpl13a,* a classical housekeeping gene, encodes a protein component of the 60S ribosomal subunit and it constitutively expressed [42–45]. It has been identified as one of the most stably expressed housekeeping genes in the liver of a diabetic mouse model [46]. *Rpl13a* also has been shown to be expressed at relatively stable levels and has been used as an internal reference gene for RT-qPCR in the spleen, a tissue rich in B cells, T cells, macrophages and dendritic cells, among other immune cell populations [47]. *Tubb2a*, a member of the β-tubulin IIa class family that constitutes a core component of the microtubule cytoskeleton, has been employed as an internal control gene in epithelial brushings collected from patients with asthma [48].

Although several stably expressed genes were commonly identified across the different tissues of *E. multilocularis*-infected mice, no gene was found to be universally unstable. Hence, the unstable expressed genes identified in this study were tissue-specific, and their expression variations may be associated with the pathological characteristics of the respective tissues. In echinococcosis, parasite induces significant pathological changes across multiple host tissues, including mechanical damage, inflammatory response, and fibrosis surrounding the parasitized lesions [49–51], as well as systemic pathological effects [52,53]. Consequently, the expression of certain conventionally recognized housekeeping genes can also be disturbed. As the primary lesion location, the liver exhibits severe damage, particularly in the perilesional area, where intense inflammatory responses are observed [54]. Accordingly, *Rplp0*, *Gapdh*, *Hprt*, and *Rn18s* failed to exhibit stable expression in the liver parasitized by *E.multilocularis*. *Rplp0* is a ribosomal protein located in the P-stalk region of the 60S large subunit, a highly dynamic domain that may render its expression more susceptible to stimuli. The inflammatory stress surrounding lesions in the liver may further exacerbate this instability by disrupting ribosomal function [55,56]. Notably, the expression of *Rplp0* was significantly upregulated in multiple cancer types, underscoring its context-dependent regulation [57,58]. *Gapdh* is a multifunctional enzyme that catalyzes a key step in glycolysis while also participating in DNA repair, gene regulation, and apoptosis, and it is commonly used as a reference gene in liver tissues

Table 3
Reference gene stability rankings across different algorithms in tissues of *E. multilocularis*-infected and healthy mice (unstratified analysis).

Tissue	NormFinder		GeNorm		BestKeeper		Delta-Ct		Consensus		Best combination of two genes
	Gene	Stability Value	Gene	Stability Value	Gene	SD	Gene	SD	Gene	Geomean of ranking values	
Liver	*Rpl13a*	0.38	*Ppia*	0.42	*Actb*	0.62	*Rpl13a*	0.85	*Tuba*	2.06	*Tuba* and *Actb*
	Actb	0.38	*Tuba*	0.42	*Tuba*	0.65	*Actb*	0.86	*Actb*	2.11	
	Tuba	0.40	*Rpl13a*	0.57	*Ppia*	0.73	*Tuba*	0.87	*Rpl13a*	2.21	
	Gusb	0.42	*Gusb*	0.62	*Mrpl32*	0.73	*Gusb*	0.88	*Ppia*	2.94	
	Ppia	0.50	*Actb*	0.65	*Gapdh*	0.77	*Ppia*	0.91	*Gusb*	4.60	
	β2m	0.60	*β2m*	0.66	*Rplp0*	0.79	*β2m*	0.96	*Gapdh*	6.44	
	Gapdh	0.73	*Gapdh*	0.74	*Gusb*	0.83	*Gapdh*	1.06	*β2m*	6.64	
	Rplp0	0.95	*Hprt*	0.82	*Rpl13a*	0.84	*Rplp0*	1.19	*Rplp0*	7.67	
	Hprt	0.97	*Rplp0*	0.87	*β2m*	0.85	*Hprt*	1.19	*Mrpl32*	8.54	
	Tubb2a	1.03	*Tubb2a*	0.92	*Rn18s*	0.93	*Tubb2a*	1.23	*Hprt*	9.39	
	Mrpl32	1.10	*Mrpl32*	0.99	*Tubb2a*	0.96	*Mrpl32*	1.29	*Tubb2a*	10.24	
	Rn18s	1.20	*Rn18s*	1.05	*Hprt*	1.12	*Rn18s*	1.36	*Rn18s*	11.47	
Lung	*Actb*	0.46	*Tuba*	0.46	*Tubb2a*	0.70	*Actb*	1.34	*Actb*	1.63	*Actb* and *Tubb2a*
	Tubb2a	0.57	*Actb*	0.46	*Ppia*	0.74	*Tubb2a*	1.39	*Tubb2a*	1.86	
	Tuba	0.73	*Tubb2a*	0.55	*Mrpl32*	0.79	*Tuba*	1.40	*Tuba*	2.71	
	Rpl13a	0.85	*Rplp0*	0.66	*Rpl13a*	0.94	*Rplp0*	1.51	*Rplp0*	4.47	
	Rplp0	1.11	*Mrpl32*	0.70	*Rplp0*	0.98	*Rpl13a*	1.52	*Rpl13a*	4.68	
	Mrpl32	1.17	*Rpl13a*	0.74	*Tuba*	0.99	*Mrpl32*	1.57	*Mrpl32*	4.82	
	Ppia	1.46	*Gapdh*	0.80	*Actb*	0.99	*Gapdh*	1.75	*Ppia*	5.47	
	Gapdh	1.49	*Ppia*	0.88	*Gapdh*	1.11	*Ppia*	1.81	*Gapdh*	7.48	
	Rn18s	1.65	*Rn18s*	1.21	*Rn18s*	1.77	*Rn18s*	2.11	*Rn18s*	9.00	
	Gusb	1.88	*Gusb*	1.46	*Gusb*	2.10	*Gusb*	2.20	*Gusb*	10.00	
	Hprt	2.15	*Hprt*	1.66	*β2m*	2.55	*Hprt*	2.42	*Hprt*	11.24	
	β2m	2.23	*β2m*	1.79	*Hprt*	2.65	*β2m*	2.45	*β2m*	11.74	
Spleen	*Rpl13a*	0.18	*Ppia*	0.25	*Tuba*	0.35	*Actb*	1.08	*Actb*	2.28	*Actb* and *Mrpl32*
	Tuba	0.57	*Mrpl32*	0.25	*Rpl13a*	0.37	*Mrpl32*	1.09	*Mrpl32*	2.51	
	Actb	0.71	*Actb*	0.27	*Actb*	0.52	*Ppia*	1.09	*Tuba*	2.89	
	Mrpl32	0.78	*Rplp0*	0.30	*Rplp0*	0.53	*Rplp0*	1.11	*Rpl13a*	3.13	
	Rplp0	0.78	*Gapdh*	0.33	*Mrpl32*	0.53	*Tuba*	1.13	*Ppia*	3.22	
	Ppia	0.82	*Tubb2a*	0.38	*Ppia*	0.58	*Rpl13a*	1.13	*Rplp0*	4.23	
	Tubb2a	0.92	*Tuba*	0.46	*Gapdh*	0.67	*Tubb2a*	1.21	*Gapdh*	6.88	
	Gapdh	1.02	*Rpl13a*	0.55	*Tubb2a*	0.75	*Gapdh*	1.23	*Tubb2a*	6.96	
	Hprt	1.25	*Hprt*	0.82	*Gusb*	1.31	*Hprt*	1.67	*Hprt*	9.24	
	Gusb	1.56	*Gusb*	1.06	*Hprt*	1.36	*Gusb*	1.83	*Gusb*	9.74	
	Rn18s	1.63	*Rn18s*	1.22	*Rn18s*	1.42	*Rn18s*	1.92	*Rn18s*	11.00	
	β2m	2.13	*β2m*	1.40	*β2m*	1.81	*β2m*	2.27	*β2m*	12.00	

Table 4
NormFinder-based reference gene stability rankings in tissues of *E. multilocularis*-infected and healthy mice (stratified analysis).

Rank	Liver (NT vs. PLT)		Liver (NT vs. DT)		Liver (PLT vs. DT)		Liver (NT vs. PLT vs. DT)		Lung (NT vs. IT)		Spleen (NT vs. IT)	
	Gene	Stability Value	Gene	Stability Value	Gene	Stability Value	Gene	Stability Value	Gene	Stability Value	Gene	Stability Value
1	*Actb*	0.16	*Rpl13a*	0.10	*Rpl13a*	0.08	*Actb*	0.16	*Actb*	0.29	*Rpl13a*	0.10
2	*Rpl13a*	0.25	*Actb*	0.13	*Ppia*	0.09	*Rpl13a*	0.20	*Tubb2a*	0.30	*Tuba*	0.16
3	*Gusb*	0.26	*Gusb*	0.13	*Tuba*	0.10	*Gusb*	0.22	*Tuba*	0.32	*Actb*	0.20
4	*Tuba*	0.29	*Tuba*	0.13	*Actb*	0.12	*Tuba*	0.22	*Rpl13a*	0.40	*Mrpl32*	0.21
5	*Ppia*	0.31	*β2m*	0.14	*Gusb*	0.14	*Ppia*	0.23	*Rplp0*	0.54	*Ppia*	0.22
6	*β2m*	0.32	*Rn18s*	0.17	*Rplp0*	0.17	*β2m*	0.25	*Mrpl32*	0.57	*Rplp0*	0.23
7	*Gapdh*	0.38	*Ppia*	0.18	*β2m*	0.19	*Gapdh*	0.29	*Rn18s*	0.58	*Tubb2a*	0.23
8	*Tubb2a*	0.44	*Mrpl32*	0.20	*Gapdh*	0.21	*Tubb2a*	0.33	*Ppia*	0.59	*Gapdh*	0.27
9	*Mrpl32*	0.51	*Tubb2a*	0.21	*Hprt*	0.24	*Rplp0*	0.33	*Gapdh*	0.64	*Hprt*	0.34
10	*Hprt*	0.51	*Gapdh*	0.23	*Tubb2a*	0.32	*Hprt*	0.35	*Gusb*	0.73	*Rn18s*	0.40
11	*Rn18s*	0.55	*Rplp0*	0.23	*Mrpl32*	0.33	*Mrpl32*	0.37	*Hprt*	0.79	*Gusb*	0.41
12	*Rplp0*	0.56	*Hprt*	0.24	*Rn18s*	0.35	*Rn18s*	0.39	*β2m*	0.81	*β2m*	0.61
Best Combination of Two Genes	*Rpl13a* and *Gusb*		*Rpl13a* and *Actb*		*Rpl13a* and *Actb*		*Tuba* and *Rpl13a*		*Tuba* and *Actb*		*Tuba* and *Rpl13a*	

under various disease conditions, including *Echinococcus* infection [27,28,59,60]. However, our results demonstrated its instability in the liver of *E. multilocularis*-infected mice, indicating that it is not suitable as an internal control gene in this disease model. Moreover, *Hprt,* a key enzyme in purine metabolism, is sensitive to alterations in cellular metabolic states induced by tumors and neurodegenerative diseases [61,62].

In spleen and lung tissues, *β2m*, *Gusb*, *Rn18s*, and *Hprt* showed poor stability. As a key immune organ in the host responding to infection, the spleen undergoes progressive enlargement as the disease advances, and the abundance and polarization state of immune cells such as macrophages dynamically change over the course of infection, shifting from an early pro-inflammatory (M1-dominated) response toward a Th2/Treg-associated immunosuppressive (M2-dominated) microenvironment

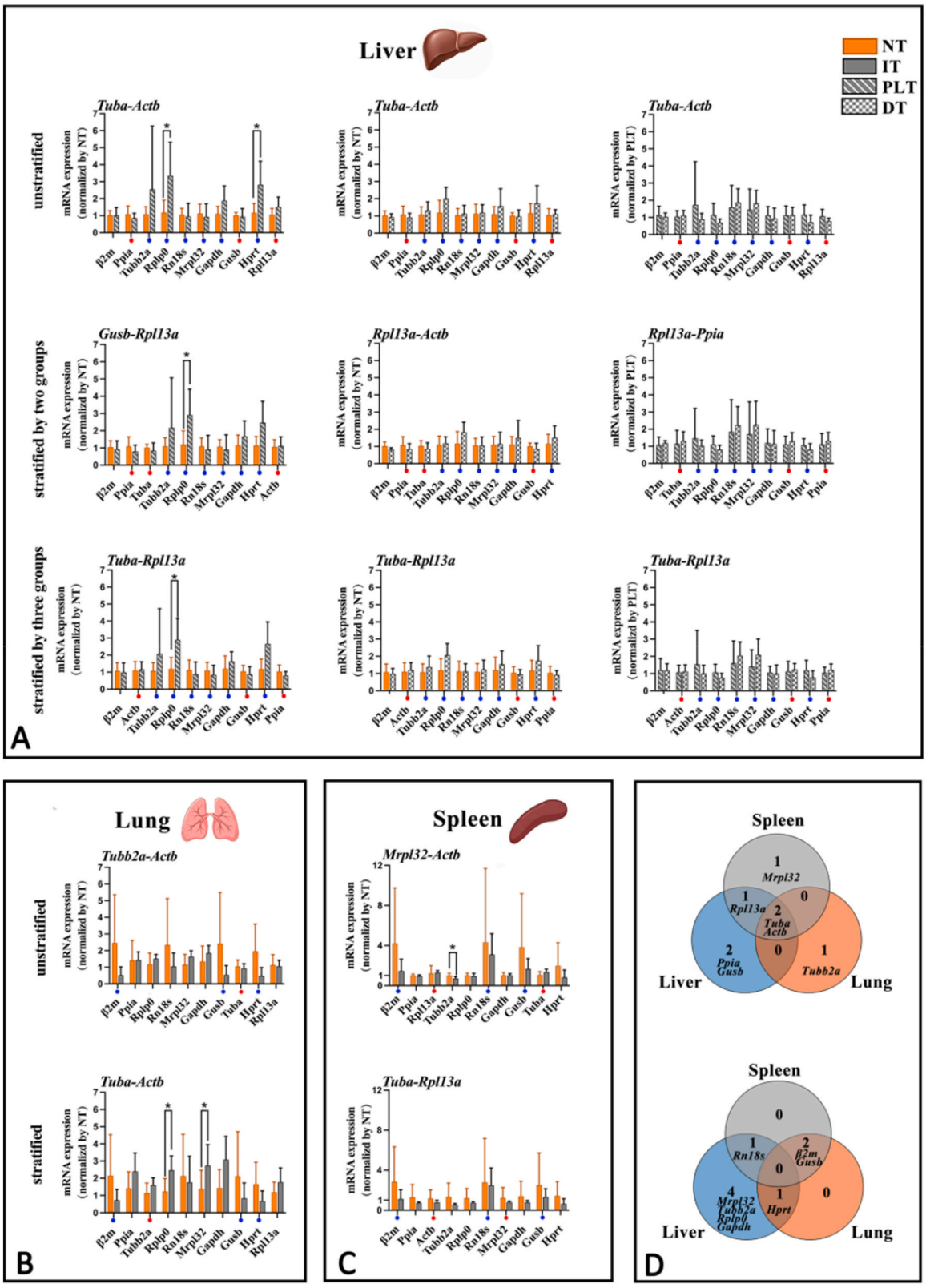

Fig. 4. Expression profiling of housekeeping genes in tissues of *E. multilocularis*-infected mice. Relative expression of housekeeping genes in liver (A), lung (B), and spleen (C) tissues during *E. multilocularis* infection, using reference combinations recommended by unstratified and stratified analysis. Red dots: genes ranked among the top three most stable reference genes, under unstratified consensus ranking or stratified analysis. Blue dots: genes ranked among the bottom three least stable reference genes, under unstratified consensus ranking or stratified analysis. Data are presented as Mean ± SD. * indicates $P < 0.05$. D. Venn graph of most (upper) and least (lower) stable genes in different tissues of mice under *E. multilocularis* infection. Genes ranked among the top or bottom three most stable reference genes under unstratified consensus ranking or stratified analysis were included.

during the chronic phase, which may destabilize the expression of *β2m* (immune-related) and *Hprt* (metabolic-related) at different infection stages [63–65]. Although studies on these genes in the lung remain limited, their unstable expression renders them unsuitable as internal controls in this tissue.

Several limitations should be acknowledged in the present study. First, the sample size used in the present study was relatively modest, but the complex host-parasite interactions during *E. multilocularis* infection may introduce considerable inter-individual variability, which could affect the stability rankings for candidate reference genes. Second, this study focused on a single disease stage, given that the host immune microenvironment undergoes dynamic remodeling throughout infection, additional investigations encompassing other stages are warranted to validate the broader applicability of the recommended reference gene combinations.

5. Conclusion

By integrating algorithmic rankings with experimental validation, optimal reference gene combinations for RT-qPCR detection of gene expression in different tissue types of mice infected with *E. multilocularis* were recommended. It provides accurate normalization and reliable quantification of target gene expression in *E. multilocularis* infection studies and will facilitate future studies in echinococcosis, including disease pathogenesis, antiparasitic drug efficacy assessment, and therapeutic target discovery.

CRediT authorship contribution statement

Rui Chen: Writing – original draft, Visualization, Methodology, Formal analysis, Data curation. **Meng Yin:** Supervision, Methodology. **Jian Xue:** Writing – review & editing. **Jianhai Yin:** Writing – review & editing, Conceptualization. **Hua Liu:** Writing – review & editing, Supervision. **Congshan Liu:** Writing – review & editing, Funding acquisition, Conceptualization.

Ethics statement

Animal procedures were carried out in compliance with the Guidelines for the Care and Use of Laboratory Animals produced by the Shanghai Veterinary Research Institute. The study was approved by the Ethics Committee of the National Institute of Parasitic Diseases, Chinese Center for Disease Control and Prevention (license number: IPD-2024-019).

Funding

This study was funded by the Natural Science Foundation of Shanghai (grant 24ZR1473300).

Declaration of competing interests

The authors declare the following financial interests/personal relationships which may be considered as potential competing interests: Congshan reports financial support was provided by Natural Science Foundation of Shanghai. If there are other authors, they declare that they have no known competing financial interests or personal relationships that could have appeared to influence the work reported in this paper.

Appendix A. Supplementary data

Supplementary data to this article can be found online at https://doi.org/10.1016/j.micpath.2026.108809.

Data availability

Data will be made available on request.

References

[1] B. Lundström-Stadelmann, A. Rostami, C.F. Frey, P.R. Torgerson, S.M. Riahi, K. Bagheri, et al., Human alveolar echinococcosis-global, regional, and national annual incidence and prevalence rates, Clin. Microbiol. Infect. 31 (2025) 1139–1145, https://doi.org/10.1016/j.cmi.2025.01.034.
[2] H. Wen, L. Vuitton, T. Tuxun, J. Li, D.A. Vuitton, W. Zhang, et al., Echinococcosis: advances in the 21st century, Clin. Microbiol. Rev. 32 (2019), https://doi.org/10.1128/cmr.00075-18.
[3] N. Badwaik, P. Gharde, R.K. Shinde, H. Tayade, P.S. Navandhar, M. Patil, Hydatid cyst or echinococcosis: a comprehensive review of transmission, clinical manifestations, diagnosis, and multidisciplinary treatment, Cureus 16 (2024) e63713, https://doi.org/10.7759/cureus.63713.
[4] D.M. Smith, L.S. Rickman, Echinococcosis: a drop of water—review on human disease, diagnosis, and management, Infect. Dis. Clin. Pract. 10 (2001) 355–359.
[5] M. Sarkar, R. Pathania, A. Jhobta, B.R. Thakur, R. Chopra, Cystic pulmonary hydatidosis, Lung India 33 (2016) 179–191, https://doi.org/10.4103/0970-2113.177449.
[6] A.L. Taratuto, S.M. Venturiello, Echinococcosis, Brain Pathol. 7 (1997) 673–679, https://doi.org/10.1111/j.1750-3639.1997.tb01082.x.
[7] M. Conchedda, A. Antonelli, A. Caddori, F. Gabriele, A retrospective analysis of human cystic echinococcosis in Sardinia (Italy), an endemic Mediterranean region, from 2001 to 2005, Parasitol. Int. 59 (2010) 454–459, https://doi.org/10.1016/j.parint.2010.06.008.
[8] M. Jallali, M.A. Chaouch, H. Zenati, H.B. Hassine, J. Saad, F. Noomen, Primary isolated hydatid cyst of the spleen: a case report, Int. J. Surg. Case Rep. 117 (2024) 109552, https://doi.org/10.1016/j.ijscr.2024.109552.
[9] L. Peters, S. Burkert, B. Grüner, Parasites of the liver - epidemiology, diagnosis and clinical management in the European context, J. Hepatol. 75 (2021) 202–218, https://doi.org/10.1016/j.jhep.2021.02.015.
[10] L.A. Salm, A. Lachenmayer, S.F. Perrodin, D. Candinas, G. Beldi, Surgical treatment strategies for hepatic alveolar echinococcosis, Food Waterborne Parasitol 15 (2019) e00050, https://doi.org/10.1016/j.fawpar.2019.e00050.
[11] F. Mohammadnejad, F. Ghaffarifar, A. Dalimi, Z.M. Hassan, The development of new treatment options for echinococcosis, Reviews and Research in Medical Microbiology 26 (2015) 154–162, https://doi.org/10.1097/mrm.0000000000000058.
[12] J. El-On, Benzimidazole treatment of cystic echinococcosis, Acta Trop. 85 (2003) 243–252, https://doi.org/10.1016/s0001-706x(02)00217-6.
[13] D. Bong, J. Sohn, S.-J.V. Lee, Brief guide to RT-qPCR, Mol. Cells 47 (2024) 100141, https://doi.org/10.1016/j.mocell.2024.100141.
[14] C. Zhang, J. Wang, G. Lü, J. Li, X. Lu, G. Mantion, et al., Hepatocyte proliferation/growth arrest balance in the liver of mice during E. multilocularis infection: a coordinated 3-stage course, PLoS One 7 (2012) e30127, https://doi.org/10.1371/journal.pone.0030127.
[15] J.A. Loos, M. Franco, M. Chop, C. Rodriguez Rodrigues, A.C. Cumino, Resveratrol against echinococcus sp.: discrepancies between in vitro and in vivo responses, Trop. Med. Infect. Dis. 8 (2023), https://doi.org/10.3390/tropicalmed8100460.
[16] J. Huggett, K. Dheda, S. Bustin, A. Zumla, Real-time RT-PCR normalisation; strategies and considerations, Gene Immun. 6 (2005) 279–284, https://doi.org/10.1038/sj.gene.6364190.
[17] K.F. Tung, C.Y. Pan, W.C. Lin, Housekeeping protein-coding genes interrogated with tissue and individual variations, Sci. Rep. 14 (2024) 12454, https://doi.org/10.1038/s41598-024-63269-4.
[18] H.J. Kim, J.I. Na, B.W. Min, J.Y. Na, K.H. Lee, J.H. Lee, et al., Evaluation of protein expression in housekeeping genes across multiple tissues in rats, Korean J Pathol 48 (2014) 193–200, https://doi.org/10.4132/KoreanJPathol.2014.48.3.193.
[19] H. Gong, L. Sun, B. Chen, Y. Han, J. Pang, W. Wu, et al., Evaluation of candidate reference genes for RT-qPCR studies in three metabolism related tissues of mice after caloric restriction, Sci. Rep. 6 (2016) 38513, https://doi.org/10.1038/srep38513.
[20] A. Secio-Silva, F. Emrich, P.H. Evangelista-Silva, R.P. Prates, A.H.T. Hijo, T. N. Figueira-Costa, et al., Which housekeeping gene is the best choice for RT-qPCR analysis in mice fed with a high-fat diet? Studies in the liver, kidney, pancreas, and intestines, Gene Reports 31 (2023) 101756, https://doi.org/10.1016/j.genrep.2023.101756.
[21] J.L.N. Souza, C.A. Lopes, T. Leal-Silva, F. Vieira-Santos, C.C.O. Amorim, L.L. S. Padrão, et al., Evaluation of reference genes for gene expression analysis by real-time quantitative PCR (qPCR) in different tissues from mice infected by Ascaris suum, Microb. Pathog. 189 (2024) 106567, https://doi.org/10.1016/j.micpath.2024.106567.
[22] A. Kalyanasundaram, B.J. Henry, C. Henry, J. Leach, R.J. Kendall, Selection of suitable reference genes for normalization of RT-qPCR in three tissues of Northern bobwhite (Colinus virginianus) infected with eyeworm (Oxyspirura petrowi), Mol. Biol. Rep. 51 (2024) 483, https://doi.org/10.1007/s11033-024-09401-z.
[23] C.L. Andersen, J.L. Jensen, T.F. Ørntoft, Normalization of real-time quantitative reverse transcription-PCR data: a model-based variance estimation approach to identify genes suited for normalization, applied to bladder and colon cancer data sets, Cancer Res. 64 (2004) 5245–5250, https://doi.org/10.1158/0008-5472.Can-04-0496.

[24] J. Vandesompele, K. De Preter, F. Pattyn, B. Poppe, N. Van Roy, A. De Paepe, et al., Accurate normalization of real-time quantitative RT-PCR data by geometric averaging of multiple internal control genes, Genome Biol. 3 (2002) Research0034, https://doi.org/10.1186/gb-2002-3-7-research0034.
[25] M.W. Pfaffl, A. Tichopad, C. Prgomet, T.P. Neuvians, Determination of stable housekeeping genes, differentially regulated target genes and sample integrity: BestKeeper–Excel-based tool using pair-wise correlations, Biotechnol. Lett. 26 (2004) 509–515, https://doi.org/10.1023/b:bile.0000019559.84305.47.
[26] K.J. Livak, T.D. Schmittgen, Analysis of relative gene expression data using real-time quantitative PCR and the 2(-Delta Delta C(T)) Method, Methods 25 (2001) 402–408, https://doi.org/10.1006/meth.2001.1262.
[27] Y.J. Yin, Q. Zhang, Y.X. Yang, S.K. Yang, H.F. Wang, J.X. Shi, et al., Study of the genes correlated with cyst calcification in patients with cystic echinococcosis, Zhonghua Yufang Yixue Zazhi 50 (2016) 434–438, https://doi.org/10.3760/cma.j.issn.0253-9624.2016.05.009.
[28] T. Tuxun, H.Z. Ma, S. Apaer, H. Zhang, A. Aierken, Y.P. Li, et al., Expression of toll-like receptors 2 and 4 and related cytokines in patients with hepatic cystic and alveolar echinococcosis, Mediat. Inflamm. 2015 (2015) 632760, https://doi.org/10.1155/2015/632760.
[29] R. Lin, G. Lü, J. Wang, C. Zhang, W. Xie, X. Lu, et al., Time course of gene expression profiling in the liver of experimental mice infected with Echinococcus multilocularis, PLoS One 6 (2011) e14557, https://doi.org/10.1371/journal.pone.0014557.
[30] Y. Chen, H.J. Gao, C. Li, X.J. Mo, G.R. Zheng, J. Xie, et al., MicroRNA expression dynamics in mouse liver at different stages of Echinococcus multilocularis infection, BMC Genom. 26 (2025) 941, https://doi.org/10.1186/s12864-025-12049-z.
[31] C. Liu, J. Cao, H. Zhang, M.C. Field, J. Yin, Extracellular vesicles secreted by Echinococcus multilocularis: important players in angiogenesis promotion, Microb. Infect. 25 (2023) 105147, https://doi.org/10.1016/j.micinf.2023.105147.
[32] M.W. Pfaffl, A new mathematical model for relative quantification in real-time RT-PCR, Nucleic Acids Res. 29 (2001) e45, https://doi.org/10.1093/nar/29.9.e45.
[33] D.G. Ginzinger, Gene quantification using real-time quantitative PCR: an emerging technology hits the mainstream, Exp. Hematol. 30 (2002) 503–512, https://doi.org/10.1016/S0301-472X(02)00806-8.
[34] J. Wang, R. Lin, W. Zhang, L. Li, B. Gottstein, O. Blagosklonov, et al., Transcriptional profiles of cytokine/chemokine factors of immune cell-homing to the parasitic lesions: a comprehensive one-year course study in the liver of E. Multilocularis-infected mice, PLoS One 9 (2014) e91638, https://doi.org/10.1371/journal.pone.0091638.
[35] A. Mehta, S. Dobersch, R.H. Dammann, S. Bellusci, O.N. Ilinskaya, T. Braun, et al., Validation of Tuba1a as appropriate internal control for normalization of gene expression analysis during mouse lung development, Int. J. Mol. Sci. 16 (2015) 4492–4511, https://doi.org/10.3390/ijms16034492.
[36] C. Guo, S. Liu, J. Wang, M.Z. Sun, F.T. Greenaway, ACTB in cancer, Clin. Chim. Acta 417 (2013) 39–44, https://doi.org/10.1016/j.cca.2012.12.012.
[37] R. Qu, Y. Miao, Y. Cui, Y. Cao, Y. Zhou, X. Tang, et al., Selection of reference genes for the quantitative real-time PCR normalization of gene expression in Isatis indigotica fortune, BMC Mol. Biol. 20 (2019) 9, https://doi.org/10.1186/s12867-019-0126-y.
[38] X. Shi, Q. Zheng, X. Wang, W. Guo, Z. Lin, Y. Gao, et al., Compromised macrophages contribute to progression of MASH to hepatocellular carcinoma in FGF21KO mice, Sci. Adv. 10 (2024) eado9311, https://doi.org/10.1126/sciadv.ado9311.
[39] R. Li, Y. Shen, An old method facing a new challenge: re-visiting housekeeping proteins as internal reference control for neuroscience research, Life Sci. 92 (2013) 747–751, https://doi.org/10.1016/j.lfs.2013.02.014.
[40] X. Chen, Y. Yu, T. Gao, Z. Liu, S. Chen, Y. Jia, Determination of stable reference genes for gene expression analysis in Black rockfish (Sebastes schlegeli) under Hypoxia stress, Genes 16 (2024), https://doi.org/10.3390/genes16010009.
[41] S. Yu, H.E. Hwang, N. Yun, J.R. Goldenring, K.T. Nam, The mRNA and protein levels of tubulin and β-Actin are greatly reduced in the proximal duodenum of mice relative to the rest of the small intestines, Dig. Dis. Sci. 60 (2015) 2670–2676, https://doi.org/10.1007/s10620-015-3688-7.
[42] R. Jesnowski, C. Backhaus, J. Ringel, M. Löhr, Ribosomal highly basic 23-kDa protein as a reliable standard for gene expression analysis, Pancreatology 2 (2002) 421–424, https://doi.org/10.1159/000065091.
[43] A. Uppalapati, T. Wang, L.H. Nguyen, Evaluation of suitable reference genes for gene expression studies in the developing mouse cortex using RT-qPCR, BMC Neurosci. 26 (2025) 12, https://doi.org/10.1186/s12868-025-00934-y.
[44] Y. Luan, N. Tang, J. Yang, S. Liu, C. Cheng, Y. Wang, et al., Deficiency of ribosomal proteins reshapes the transcriptional and translational landscape in human cells, Nucleic Acids Res. 50 (2022) 6601–6617, https://doi.org/10.1093/nar/gkac053.
[45] S.S. Magadi, M. Jonson, P.B. Lucena, M.F. Caliandro, B. Almeida, L. Bilalli, et al., Neuroinflammation and neurodegeneration trigger a specific splice form of ribosomal protein S24, Brain (2026), https://doi.org/10.1093/brain/awag166.
[46] V.D. Nong, D.Q. Nguyen, T.T. Do, T.H. Giang Tran, T.H. Nguyen, T.T. Le, et al., Identification of stable internal reference genes for expression analysis in the liver and pancreas of diabetic mouse (Mus musculus L.) models under physiological, pathological and treatment conditions, PLoS One 21 (2026) e0338403, https://doi.org/10.1371/journal.pone.0338403.
[47] I.R. Peters, D. Peeters, C.R. Helps, M.J. Day, Development and application of multiple internal reference (housekeeper) gene assays for accurate normalisation of canine gene expression studies, Vet. Immunol. Immunopathol. 117 (2007) 55–66, https://doi.org/10.1016/j.vetimm.2007.01.011.
[48] T. Southworth, M. Van Geest, D. Singh, Type-2 airway inflammation in mild asthma patients with high blood eosinophils and high fractional exhaled nitric oxide, Clin. Transl. Sci. 14 (2021) 1259–1264, https://doi.org/10.1111/cts.13078.
[49] S. Greco, R. Cannella, D. Giambelluca, G. Pecoraro, E. Battaglia, M. Midiri, et al., Complications of hepatic echinococcosis: multimodality imaging approach, Insights Imaging 10 (2019) 113, https://doi.org/10.1186/s13244-019-0805-8.
[50] H. Aslam, H. Wardah, K. Akhtar, S.H. Arif, M. Irshadullah, Histologic, histochemical, and immunohistochemical changes in buffalo liver with cystic echinococcosis, Vet. Pathol. 62 (2025) 319–326, https://doi.org/10.1177/03009858241309399.
[51] R.J. Zhang, H.S. Pang, J.Z. Li, Z.H. Luo, L. Ai, P. Song, et al., Mechanism of hepatic fibrosis associated with Echinococcus: a review, Zhongguo Xue Xi Chong Bing Fang Zhi Za Zhi 34 (2022) 646–653, https://doi.org/10.16250/j.32.1374.2022178.
[52] M. Manabe, T. Nakamura, K. Sato, N. Hayashi, H. Kouguchi, R. Nakao, et al., Efferocytosis-Driven M2 macrophage impairs fibrotic encapsulation and promotes Echinococcus multilocularis growth in cotton rats (Sigmodon hispidus), Microsc. Microanal. 31 (2025), https://doi.org/10.1093/mam/ozaf082.
[53] X.X. Wu, W.L. Ban, L.J. Wu, W.J. Qi, M. Borhani, X.Y. He, et al., Identification of serum biomarkers for cystic echinococcosis in sheep through untargeted metabolomic analysis using LC-MS/MS technology, Parasites Vectors 17 (2024) 547, https://doi.org/10.1186/s13071-024-06599-6.
[54] Z. Ou, L. Li, P. Ren, T.T. Zhou, F. He, J. Chen, et al., Spatiotemporal transcriptomic profiling reveals the dynamic immunological landscape of alveolar echinococcosis, Adv. Sci. (Weinh.) 12 (2025) e2405914, https://doi.org/10.1002/advs.202405914.
[55] C. Datta, S.S. Truesdell, K.Q. Wu, S.I.A. Bukhari, H. Ngue, B. Buchanan, et al., Ribosome changes reprogram translation for chemosurvival in G0 leukemic cells, Sci. Adv. 8 (2022) eabo1304, https://doi.org/10.1126/sciadv.abo1304.
[56] A. Artero-Castro, M. Perez-Alea, A. Feliciano, J.A. Leal, M. Genestar, J. Castellvi, et al., Disruption of the ribosomal P complex leads to stress-induced autophagy, Autophagy 11 (2015) 1499–1519, https://doi.org/10.1080/15548627.2015.1063764.
[57] B. Yan, J. Guo, W. Lai, Y. Chen, Z. Wang, Y. Peng, et al., The multifaceted roles of ribosomal P complex in cancer, World J. Surg. Oncol. 23 (2025) 388, https://doi.org/10.1186/s12957-025-04014-7.
[58] C. Xu, Z. Lu, G. Hou, M. Zhu, Exploring the function and prognostic value of RPLP0, RPLP1 and RPLP2 expression in lung adenocarcinoma, J. Mol. Histol. 55 (2024) 1079–1091, https://doi.org/10.1007/s10735-024-10251-z.
[59] A. Romaniuk-Drapała, K. Kosicka-Noworzyń, Y.H. Sheng, C. Yohn, L. Brunetti, L. Kagan, Evaluation of reference genes for qPCR in human liver and kidney tissue from individuals with obesity, Sci. Rep. 15 (2025) 5347, https://doi.org/10.1038/s41598-025-87911-x.
[60] M.P. Herrera-Sánchez, K.J. Lozano-Villegas, I.S. Rondón-Barragán, R. Rodríguez-Hernández, Identification of reference genes for expression studies in the liver and spleen of laying hens housed in cage and cage-free systems, Open Vet. J. 13 (2023) 270–277, https://doi.org/10.5455/OVJ.2023.v13.i3.3.
[61] M. Garcia-Gil, M. Camici, S. Allegrini, R. Pesi, E. Petrotto, M.G. Tozzi, Emerging role of purine metabolizing enzymes in brain function and tumors, Int. J. Mol. Sci. 19 (2018), https://doi.org/10.3390/ijms19113598.
[62] Z. Wu, D. Bezwada, F. Cai, R.C. Harris, B. Ko, V. Sondhi, et al., Electron transport chain inhibition increases cellular dependence on purine transport and salvage, Cell Metab. 36 (2024), https://doi.org/10.1016/j.cmet.2024.05.014, 1504-20.e9.
[63] J. Hou, H. Wen, M.K. Wang, W.D. Li, J. Li, Changes of macrophage subsets and polarization in spleen of mice infected with Echinococcus multilocularis, Chin. J. Parasitol. Parasit. Dis. 39 (2021) 771–778, https://doi.org/10.12140/j.issn.1000-7423.2021.06.007.
[64] Z. Ali-Khan, Cellular changes in the lymphoreticular tissues of C57L/J mice infected with Echinococcus multilocularis cysts, Immunology 34 (1978) 831–839.
[65] H. Wang, C.S. Zhang, B.B. Fang, J. Hou, W.D. Li, Z.D. Li, et al., Dual role of hepatic macrophages in the establishment of the Echinococcus multilocularis metacestode in mice, Front. Immunol. 11 (2020) 600635, https://doi.org/10.3389/fimmu.2020.600635.